Efficient current-induced magnetization reversal by spin-orbit torque in Pt/Co/Pt

R. M. Rowan-Robinson, A. T. Hindmarch, and D. Atkinson

Citation: Journal of Applied Physics **124**, 183901 (2018); doi: 10.1063/1.5046503
View online: https://doi.org/10.1063/1.5046503
View Table of Contents: http://aip.scitation.org/toc/jap/124/18
Published by the American Institute of Physics

JOURNAL OF APPLIED PHYSICS **124**, 183901 (2018)

Efficient current-induced magnetization reversal by spin-orbit torque in Pt/Co/Pt

R. M. Rowan-Robinson,[a] A. T. Hindmarch, and D. Atkinson[b]
Department of Physics, Durham University, South Road, Durham DH1 3LE, United Kingdom

(Received 28 June 2018; accepted 15 October 2018; published online 8 November 2018)

Current-induced magnetization reversal due to spin-orbit torque is demonstrated in an anisotropy controlled Pt/Co/Pt trilayer. The samples were designed to have weak perpendicular magnetic anisotropy, with a measured anisotropy field of (1340 ± 20) Oe. Reversal is shown to be dominated by a damping-like torque associated with the spin-Hall effect. A small in-plane magnetic field was required to break the symmetry and enable reversal. With a 273 Oe field, magnetization reversal occurred with a current density amplitude of only 5×10^{10} A m^{-2}, which is shown to be consistent with a simple model. The field-like torque is negligible, so measurements indicate that the imaginary part of the spin-mixing conductance associated with Co/Pt interfaces must be negligible. *Published by AIP Publishing.* https://doi.org/10.1063/1.5046503

I. INTRODUCTION

Manipulation and switching of magnetization using current-induced torques offers real opportunities for improved scalability and reduced power consumption for magnetic memory and logic devices. The first developments focused on spin-transfer torque induced via the propagation of spin-polarized current flowing perpendicularly through a magnetic multilayer[1,2] or across a magnetic domain wall.[3,4] However, the high critical current densities required ($j_c \sim 10^{12}$ Am^{-2}) remain challenging for applications requirements.[5] So, recent attention has shifted to simpler heavy metal (HM)/ferromagnet (FM) bilayers, where in-plane current can be used to manipulate chiral domain-walls[6–8] or magnetization[9,10] through spin-orbit torques (SOTs).

Spin-torques act on the magnetization with "field-like (FL)" and/or "damping-like (DL)" symmetry. The damping-like torque takes the form $\boldsymbol{\tau}_{\mathrm{DL}} \sim \boldsymbol{m} \times (\boldsymbol{m} \times \boldsymbol{\sigma})$ and is quadratic in the magnetization, whereas the field-like torque takes the form $\boldsymbol{\tau}_{\mathrm{DL}} \sim \boldsymbol{m} \times \boldsymbol{\sigma}$. Here, $\boldsymbol{\sigma}$ and $\boldsymbol{m}$ are unit vectors for the spin-current polarization in the HM layer and magnetization in the FM layer, respectively.

When the measurement timescale is much shorter than the precessional dynamics, an effective field representation is often used,[8,11–13] by which the torques are replaced with two orthogonal effective magnetic fields as illustrated in Figs. 1(a) and 1(b). The effective field associated with the field-like (FL) torque has the expression $\boldsymbol{H}_{\mathrm{FL}} \sim \hat{\boldsymbol{z}} \times \boldsymbol{j}_e$. Likewise, for the damping-like (DL) torque the effective field becomes $\boldsymbol{H}_{\mathrm{DL}} \sim \boldsymbol{m} \times (\hat{\boldsymbol{z}} \times \boldsymbol{j}_e)$, where $\hat{\boldsymbol{z}}$ is the unit vector normal to the film, $\boldsymbol{j}_e$ is the charge-current density, and $\boldsymbol{\sigma} \sim \hat{\boldsymbol{z}} \times \boldsymbol{j}_e$.

The physical phenomena underlying these SOTs have come under intense scrutiny. After some debate, it is now accepted that the DL SOT arises primarily as a result of the spin-Hall effect[6] and the transparency of the interface to the transmission of spin-current, described by the real part of the interfacial spin-mixing conductance Re$[g_{\uparrow\downarrow}]$.[12] The FL SOT, on the other hand, remains less well understood in metallic ferromagnetic systems and has been suggested to be the result of several mechanisms. First, in material combinations where the imaginary part of the spin-mixing conductance Im$[g_{\uparrow\downarrow}]$ is non-negligible, the spin-Hall effect has been proposed as a possible mechanism.[12] In systems with structural inversion asymmetry, the Rashba effect[14,15] or related inverse spin-galvanic effect (ISGE)[16] has been proposed. In very pure systems with low disorder, a "spin-swapping" mechanism has also been considered.[17]

For technological applications of SOTs, a reduction in the critical current-density for full current-induced magnetization reversal (CIMR) is required. Full reversal mediated by SOT was observed in Pt/Co/MgO structures with perpendicular magnetic anisotropy (PMA), with a critical current $j_c = 4 \times 10^{11}$ A m^{-2}[18] and for Pt/Co/AlO$_x$ structures with $j_c \sim 2.3 \times 10^{11}$ A m^{-2}.[19] More recently, work on PMA systems has shown electrical control of CIMR using a transverse bias current in Pt/Co/MgO ($j_c \sim 7.5 \times 10^{11}$ A m^{-2}),[20] full CIMR in Pd/Co/AlO$_x$ ($j_c \sim 5 \times 10^{11}$ A m^{-2}),[21] *partial* reversal in Pt/Co/Pd from a multi-domain to a saturated state by SOT ($j_c \sim 5 \times 10^{10}$ A m^{-2}),[22] and most significantly, *full* CIMR in Pt/Co/Ni/Co multilayers with the addition of Ru spin-reflecting layers to enhance the SOT by constraining the spin-current within the FM layer ($j_c \sim 5 \times 10^{10}$ A m^{-2}); however, this latter approach requires a relatively large biasing magnetic field of order 1 kOe.[23] This work presents a detailed study of SOT-driven CIMR in a carefully designed Pt/Co/Pt trilayer system with weak PMA. The results and analysis show negligible $\boldsymbol{H}_{\mathrm{FL}}$ and a simple model in which $\boldsymbol{H}_{\mathrm{DL}}$ results from the spin-Hall effect reproduce the measured critical current density for CIMR using reasonable parameters. *Full* CIMR is demonstrated with current-density amplitudes as low as 5×10^{10} A m^{-2} in the presence of a small bias field.

[a]Present address: Uppsala University; electronic mail: richard.rowan-robinson@physics.uu.se
[b]del.atkinson@durham.ac.uk

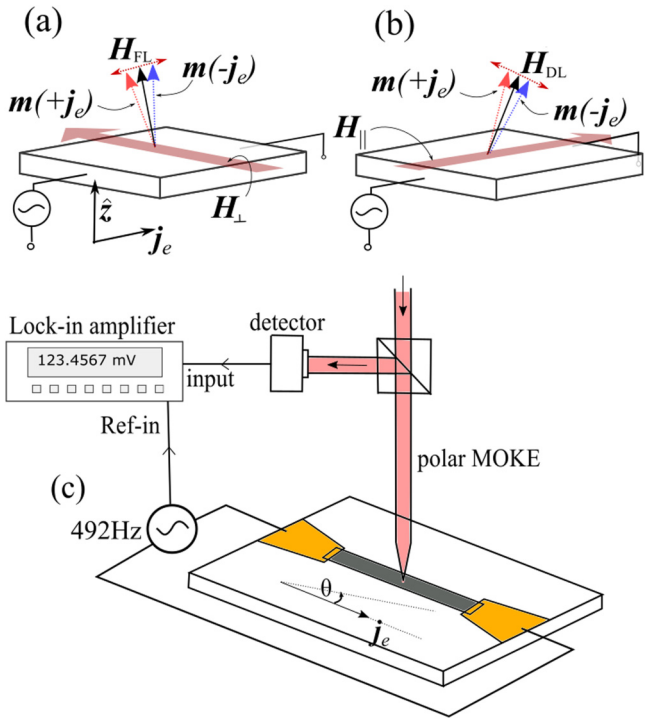

FIG. 1. Schematic illustrations of the orientations of the effective fields (a) $\boldsymbol{H}_{FL}$ and (b) $\boldsymbol{H}_{DL}$ due to SOTs, relative to the direction of the current density j_e. The magnetization at zero, positive, and negative current polarity is represented by the black, red, and blue arrows, respectively. (c) The sample structure and experimental setup.

II. EXPERIMENTAL

A polycrystalline trilayer sample with nominal layer structure Pt[1 nm]/Co[0.6 nm]/Pt[5 nm] was deposited onto an oxide-coated Si wafer substrate by DC magnetron sputtering in an ultra-high vacuum deposition system. From this film, 400 μm × 30 μm strips and electrical contacts were fabricated by photolithography.

The experimental arrangement for measuring SOTs in samples with PMA is shown in Fig. 1(c). The flow of current through the sample acted to move the magnetization away from the out-of-plane axis. An alternating current at 492 Hz was passed through the sample, causing the magnetization to oscillate about the out-of-plane axis, which was detected using the polar Kerr effect with lock-in detection, as in Ref. 11. The focused laser spot with diameter ~5 μm was positioned in the center of the wire in order to minimize any contribution from the wire edges, where the domain nucleation field could be lower (see supplementary material). The amplitude of the first harmonic of the voltage (C_ω) represents the magnitude of the polar Kerr oscillation resulting from the alternating current excitation.

The application of a static in-plane magnetic field during these alternating current measurements biases the magnetization oscillation along one axis, allowing separation of the spin-orbit torque terms, $\boldsymbol{H}_{DL}$ and $\boldsymbol{H}_{FL}$.[11,24–26] Measurements were performed in which the angle θ between current flow and in-plane magnetic bias field was varied [see Fig. 1(c)]. The angle between the in-plane field and the current flow is defined as follows: $\theta = 0°$ when the in-plane field and the current flow are parallel (longitudinal, $\boldsymbol{H}_\parallel$) and $\theta = 90°$ when the in-plane field and current flow are orthogonal (transverse, $\boldsymbol{H}_\perp$). The longitudinal field configuration is notionally sensitive only to $\boldsymbol{H}_{DL}$, while the transverse configuration is sensitive to the field-like torque, $\boldsymbol{H}_{FL}$.

III. RESULTS AND DISCUSSION

The field-driven magnetization reversal behavior of the sample was measured using polar magneto-optical Kerr effect (MOKE). The hysteresis loop shown in Fig. 2(a) demonstrates that the sample has PMA with a small coercivity of (30 ± 2) Oe. The anisotropy field, H_k, was estimated by fitting a Stoner-Wohlfarth model

$$\frac{M_z}{M_s} = \cos\left[\sin^{-1}\left(H_\parallel/H_k\right)\right]$$

to measurements of the longitudinal magnetic field dependence of the anomalous Hall effect voltage, see Fig. 2(b), where M_z is the perpendicular component of magnetization, M_s is the saturation magnetization, and $H_\parallel$ is the longitudinal field. The anisotropy field obtained with this method was $H_k = (1340 \pm 20)$ Oe. However, we emphasise that for systems with weak PMA, this method can provide only an approximate value for H_k, since it does not account for additional contributions such as domain nucleation which would cause M_z to fall more rapidly and therefore underestimate the value of H_k. This estimate of H_k indicates a weak PMA that is attributed to the thin Pt[1 nm] under-layer.

In terms of the interfaces, the trilayer sample is a nominally symmetric polycrystalline Pt/Co/Pt structure and is not expected to be in the low disorder regime to show spin-swapping transport or to exhibit any Rashba or ISGE field-like SOT contributions associated with broken symmetry. However, the thickness of the lower Pt layer is comparable with the spin-diffusion length $\lambda_{sd} \approx 1 - 2$ nm[27] in Pt, while the upper Pt (5 nm) layer is much thicker. Spin current will be generated in both Pt layers due to the spin-Hall effect but it will not cancel as the spin-current in the Co from the thicker Pt layer is expected to dominate that from the thinner Pt layer.[6] Furthermore, there would still exist an asymmetry between the Pt/Co and Co/Pt interfaces, giving rise to different proximity induced magnetization at each interface.[28] Even in the presence of symmetric Pt thicknesses, cancelation of $\boldsymbol{H}_{DL}$ would not necessarily be observed, as demonstrated in Ref. 13 for a Pt(3.5 nm)/Co(1.1 nm)/Pt(3.5 nm) film prepared on a SiO_2 substrate.

By design, this trilayer structure is expected to show *efficient CIMR* resulting from the combination of *weak PMA* and a *net spin-current* propagating into the Co layer creating an *appreciable damping-like* SOT but a *negligible field-like* SOT component.

To investigate the presence and magnitude of any $\boldsymbol{H}_{DL}$ and $\boldsymbol{H}_{FL}$ effective fields, the in-plane magnetic bias field was applied at various angles, θ, to change the relative contribution of the two torque terms on the orientation of the magnetization. Changes induced in the magnetization orientation are described by the normalized Kerr signal, C_ω/C_0, where C_0 is obtained with magnetization saturated out-of-the-plane.

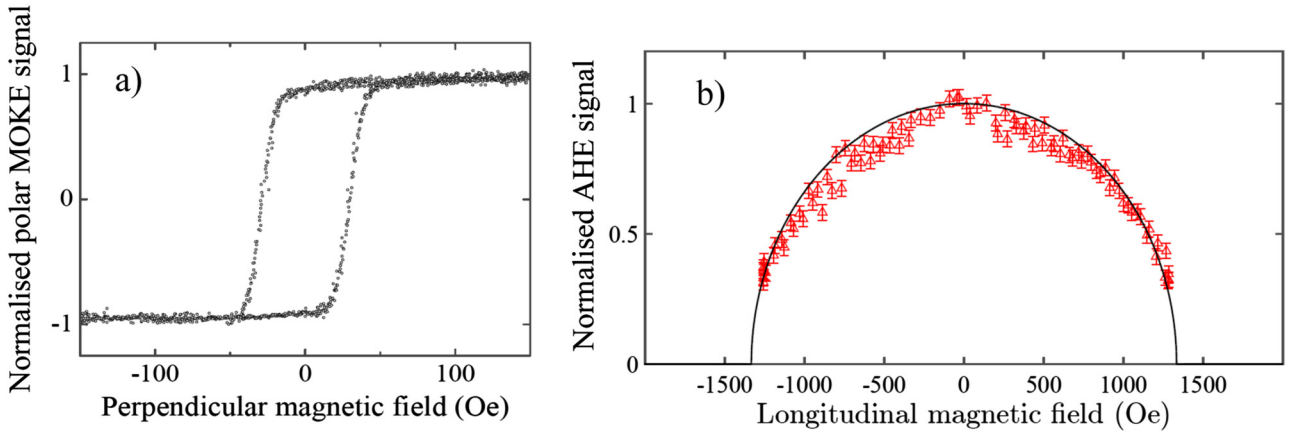

FIG. 2. (a) Polar MOKE hysteresis loop for the patterned Pt(1 nm)/Co(0.6 nm)/Pt(5 nm) trilayer sample, showing PMA with low coercivity. (b) Polar magnetization component as a function of longitudinal applied field measured using the anomalous Hall effect. The solid line in (b) is a fit to the Stoner-Wohlfarth model described in the text.

Figure 3(a) shows C_ω/C_0 as a function of in-plane field for different orientations, θ, of the field with respect to the AC current of density $j_c = 1.0 \times 10^{11}\,\mathrm{A\,m^{-2}}$. These results demonstrate that full CIMR can be achieved over a large range of applied in-plane field directions $0 < \theta \lesssim 70°$, as shown by the saturated regions, which indicate that the alternating current fully reverses the magnetization for each current polarity, i.e., $|C_\omega/C_0| = 1$. The phase of the signal undergoes a 180° change when the field polarity is reversed (see supplementary material). The magnetic field required to achieve saturation increases with increasing θ indicating that the longitudinal configuration, field and current parallel, provides the most efficient reversal regime. For $\theta = 90°$, there is almost no change in the magnetization orientation, $C_\omega/C_0 \sim 0$, indicating that $\boldsymbol{H}_{\mathrm{FL}}$ is negligibly small. Together, these results demonstrate that the $\boldsymbol{H}_{\mathrm{DL}}$ term is the dominant effective-field which is due to the predominantly damping-like SOT and supports other very recent work.[26,29]

Below, magnetic saturation C_ω/C_0 varies approximately linearly with the in-plane applied field; this gradient is proportional to the SOT and has been used to extract $\boldsymbol{H}_{\mathrm{DL}}$ and/or $\boldsymbol{H}_{\mathrm{FL}}$[11] assuming single-domain reversal. However, it is clear from the polar MOKE hysteresis loop in Fig. 2(a) and the Stoner-Wohlfarth fit to extract H_k, Fig. 2(b), that the reversal is not single domain. Nevertheless, this analytic approach can be used to compare the relative contributions of the $\boldsymbol{H}_{\mathrm{DL}}$ and $\boldsymbol{H}_{\mathrm{FL}}$ SOT terms in the region where C_ω/C_0 behaves linearly.

Figure 3(b) shows the gradient from the linear fits to the data in Fig. 3 plotted as a function of the in-plane field angle θ. For a quantitative comparison of the relative magnitudes of $\boldsymbol{H}_{\mathrm{DL}}$ and $\boldsymbol{H}_{\mathrm{FL}}$, the data were fitted with the relation $\partial(C_\omega/C_0)/\partial H = A_{\mathrm{DL}} \cos\theta + A_{\mathrm{FL}} \sin\theta$ which combines angular terms representing the $\boldsymbol{H}_{\mathrm{DL}}$ and $\boldsymbol{H}_{\mathrm{FL}}$ contributions. From this fitting, the parameters $A_{\mathrm{DL}} = (0.041 \pm 0.003)\,\mathrm{Oe^{-1}}$ and $A_{\mathrm{FL}} = (0.0000 \pm 0.0004)\,\mathrm{Oe^{-1}}$ were obtained. Within the estimated errors, only the cosine term contributes, indicating only a damping-like SOT and no field-like contribution from the SOT, confirming the absence of Rashba and/or inverse spin galvanic effects. The Oersted field would be expected to have the same symmetry as $\boldsymbol{H}_{\mathrm{FL}}$ and hence cannot explain this behavior (see supplementary material).

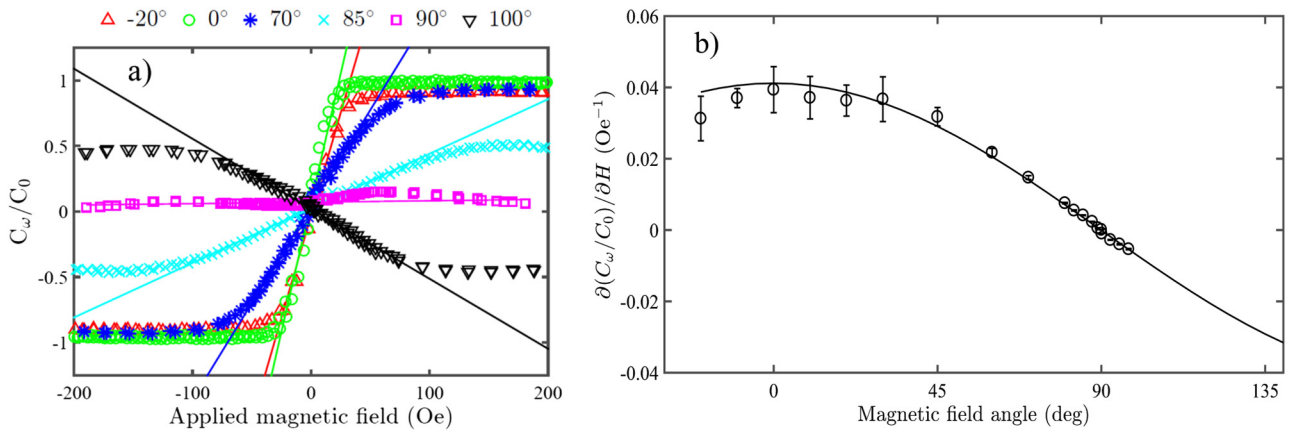

FIG. 3. (a) Polar MOKE measurements of normalized Kerr signal C_ω/C_0 as a function of the in-plane magnetic field applied at different angles θ to the AC current density, which has amplitude $j_e = 1.0 \times 10^{11}\,\mathrm{A\,m^{-2}}$. Linear fits are made in the region between $\pm 70\%$ of magnetic saturation along $\hat{z}$. (b) The gradient of the linear part of the normalized Kerr signal as a function of the in-plane field angle, θ. The solid line fit is dominated by the cosine dependence resulting from the damping-like SOT.

With the damping-like torque established, attention is turned to current-induced magnetization reversal. Examples of measured hysteresis loops as a function of alternating current density, with an amplitude of 9×10^{10} A m^{-2}, are shown for selected longitudinal bias fields $\boldsymbol{H}_{\parallel}$ in Fig. 4(a). A bias field was required to break the out-of-plane symmetry for the damping-like SOT to be effective and cause CIMR. This is supported elsewhere, as it has been shown that reversal can be mediated without an in-plane field if the symmetry is broken by alternative means.[30]

The coercivity of the current-induced loops decreased with increasing amplitude of the in-plane field. With a 273 Oe field, magnetization reversal can be achieved with a current density of 5×10^{10} A m^{-2}. The loops were offset in current which may be attributed to the Oersted field, since this does not change the direction when the magnetization is reversed; it assists the reversal process in one direction and counteracts it in the other.

With the longitudinal in-plane field, CIMR via the damping-like torque was mapped as a function of the bias field and the AC current density amplitude. The normalized Kerr signal C_ω/C_0 as a function of $\boldsymbol{H}_{\parallel}$ and AC current density amplitude is shown in Fig. 4(b). The lightest regions (yellow) correspond to full CIMR with $C_\omega/C_0 = 1$ and the darkest regions (blue), $C_\omega/C_0 \approx 0$, show the conditions for no current-induced reversal while the intermediate regions show the condition for partial CIMR. With increasing current density, $\boldsymbol{H}_{\mathrm{DL}}$ increases such that CIMR occurs with a lower in-plane bias field.

The critical current density j_c for CIMR via damping-like SOT due to the spin-Hall effect is described by[26,31,32]

$$j_c \propto \frac{\alpha M_s H_{\mathrm{eff}}}{\theta_{\mathrm{SH}}},$$

where θ_{SH} is the spin-Hall angle, α is the Gilbert damping parameter, and $H_{\mathrm{eff}} = H_k - 4\pi M_s$. Multilayers exhibiting PMA typically have large H_k, and hence, large H_{eff} which critically increases j_c. Furthermore, the Gilbert damping counteracts the damping-like torque and thus also increases j_c. It is also significant that the damping is enhanced by the combination of ultrathin ferromagnetic layers and heavy metal layers that enable PMA but depends upon the thickness of the heavy metal layer[33] and the Co thickness.[34] The α parameter can be as large as 0.4 for Pt/Co/Pt multilayers with Co thickness similar to that used here.[35]

For Co thicknesses between 3 and 10 Å in Pt/Co/Pt superlattices, M_s has been found to be between 50 and 300 emu/cm^3,[36] much lower than the bulk M_s for Co (1400 emu/cm^3). As M_s is significantly reduced when the Co layer is of sub-nanometer thickness, this could, depending on the value of H_k, act to reduce the critical current required for CIMR via DL SOT due to the spin-Hall effect.

To quantitatively test that the observed CIMR arises via a damping-like SOT due to the spin-Hall effect, the experimental value for j_c was used to estimate θ_{SH} for Pt based on the Slonczewski model[26,37,38]

$$\theta_{\mathrm{SH}} = \frac{A\alpha M_s H_{\mathrm{eff}} t_{\mathrm{FM}}}{g(\omega) j_c},$$

where t_{FM} is the ferromagnetic layer thickness, which was 0.6 nm for the Co layer in this study; A is a constant that depends on the electrical transport mechanism and takes a value of $\approx 3 \times 10^8$ A Oe^{-1}emu^{-1} for diffusive conduction;[37] and $g(\omega)$ is related to the angle ω between the spin-current polarisation and magnetization.[26,38] For spin-current resulting from the spin-Hall effect in Pt with in-plane current flow, and magnetization perpendicular to the layer plane, $\omega = 90°$, which gives $g(\omega) = 0.25$. Taking the value $M_s = 100$ emu/cm^3 as an intermediate value from Ref. 36, $\alpha = 0.4$[35] and the measured values for $H_k = 1340$ Oe and $j_c = 5 \times 10^{10}$ Am^{-2} gives a $\theta_{\mathrm{SH}} = 0.05$, which is within the range of values for the spin-Hall angle for Pt obtained by a variety of methods.[27,39,40] This agreement provides further physical evidence demonstrating that the CIMR is due to a damping-like SOT from a spin-current produced by the spin-Hall effect in the heavy metal layer.

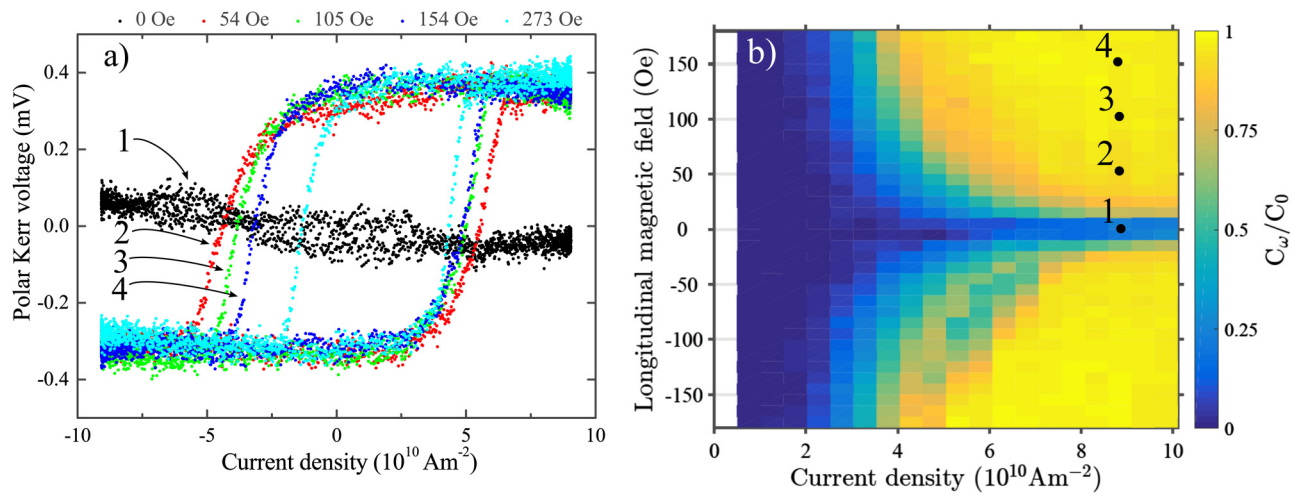

FIG. 4. (a) CIMR hysteresis loops measured using a current density amplitude of 9×10^{10} A m^{-2} AC. Each loop was measured with a static in-plane longitudinal bias field of different magnitude. (b) Switching map showing the dependence of CIMR on AC current density amplitude and in-plane bias field. The points labeled 1-4 in (b) correspond to the labeled CIMR hysteresis loops in (a).

When using this approach, the θ_{SH} obtained is a lower bound due to a partial cancelation of the spin-current from the upper and lower Pt interfaces. Furthermore, it is understood that interfacial spin-transparency makes an important contribution to the measured θ_{SH},[41] as well as the heavy metal thickness relative to the spin-diffusion length. These concepts are encapsulated within the effective spin-Hall angle, by which, in the limit that the spin-diffusion length is large compared to the heavy metal layer thickness, the effective spin-Hall angle tends to the true spin-Hall angle.

Beyond the Slonczewski model, which does not describe interfacial spin-transport in terms of spin-mixing conductance, the measurements here may also provide insight into spin-transport across NM/FM interfaces. The damping-like SOT observed here is quantitatively consistent with the spin-Hall effect mechanism and can be related to the real part of the spin-mixing conductance. Conversely, the complete absence of a field-like SOT indicates that the imaginary part of the spin-mixing conductance at the Co/Pt interfaces, which could produce a FL SOT due to spin-current arising from the spin-Hall effect, must be negligible. Thus, as predicted by theory and supported here by the measurements $\mathrm{Re}[g_{\uparrow\downarrow}] \gg \mathrm{Im}[g_{\uparrow\downarrow}]$ at Co/Pt interfaces.

IV. CONCLUSION

In summary, efficient full current-induced magnetization reversal with a very low critical current density of $5 \times 10^{10}\,\mathrm{A\,m^{-2}}$ was observed experimentally in a specifically designed Pt/Co/Pt trilayer using polar magneto-optical Kerr effect magnetometry. A small static longitudinal in-plane magnetic bias field was required to break the symmetry and allow current-induced magnetization reversal, with full reversal observed with bias fields down to 35 Oe. Analysis shows that reversal is driven entirely by a damping-like spin-orbit torque. The low critical current density for reversal results from the combination of weak perpendicular magnetic anisotropy and low saturation magnetization in the Pt/Co/Pt trilayer structure. Analysis based on the Slonczewski model and assuming that the damping-like spin-orbit torque is a result of the spin-Hall effect gave a reasonable value of 0.05 for the spin-Hall angle in platinum. Finally, this study suggests that the imaginary part of the spin-mixing conductance at cobalt/platinum interfaces is negligible.

SUPPLEMENTARY MATERIAL

See supplementary material for detailed discussions of the role of the Oersted field in these measurements as well as the phase behavior of C_ω on the longitudinal field. Also included are additional measurements demonstrating the effect of DC current on the sample as well as Kerr microscopy images of the magnetic field driven domain wall motion in the wire.

ACKNOWLEDGMENTS

The authors gratefully acknowledge EPSRC DTP studentship Reference No. 1212684 supporting RMRR. This work was also supported by EPSRC Grant Reference No. EP/L000121/1 and Durham University. The data supporting this study are available at http://dx.doi.org/10.15128/r1w0892993j.

[1]M. Tsoi, A. G. M. Jansen, J. Bass, W.-C. Chiang, M. Seck, V. Tsoi, and P. Wyder, Phys. Rev. Lett. **80**, 4281 (1998).
[2]J. A. Katine, F. J. Albert, R. A. Buhrman, E. B. Myers, and D. C. Ralph, Phys. Rev. Lett. **84**, 3149 (2000).
[3]L. Gan, S. H. Chung, K. H. Aschenbach, M. Dreyer, and R. D. Gomez, IEEE Trans. Mag. **36**, 3047 (2000).
[4]A. Yamaguchi, T. Ono, S. Nasu, K. Miyake, K. Mibu, and T. Shinjo, Phys. Rev. Lett. **92**, 077205 (2004).
[5]S. S. P. Parkin, M. Hayashi, and L. Thomas, Science **320**, 190 (2008).
[6]P. P. J. Haazen, E. Mur, J. H. Franken, R. Lavrijsen, H. J. M. Swagten, and B. Koopmans, Nat. Mater. **12**, 299 (2013).
[7]K.-S. Ryu, L. Thomas, S.-H. Yang, and S. Parkin, Nat. Nano **8**, 527 (2013).
[8]S. Emori, U. Bauer, S.-M. Ahn, E. Martinez, and G. S. D. Beach, Nat. Mater. **12**, 611 (2013).
[9]L. Liu, C.-F. Pai, Y. Li, H. W. Tseng, D. C. Ralph, and R. A. Buhrman, Science **336**, 555 (2012).
[10]G. Yu, P. Upadhyaya, Y. Fan, J. G. Alzate, W. Jiang, K. L. Wong, S. Takei, S. A. Bender, L.-t. Chang, Y. Jiang, M. Lang, J. Tang, Y. Wang, Y. Tserkovnyak, P. K. Amiri, and K. L. Wang, Nat. Nano **9**, 548 (2014).
[11]S. Emori, U. Bauer, S. Woo, and G. S. D. Beach, Appl. Phys. Lett. **105**, 222401 (2014).
[12]P. M. Haney, H.-W. Lee, K.-J. Lee, A. Manchon, and M. D. Stiles, Phys. Rev. B **87**, 174411 (2013).
[13]H. An, H. Nakayama, Y. Kanno, A. Nomura, S. Haku, and K. Ando, Phys. Rev. B **94**, 214417 (2016).
[14]Y. A. Bychkov and E. I. Rashba, JETP Lett. **39**, 78 (1984).
[15]A. Manchon and S. Zhang, Phys. Rev. B **78**, 212405 (2008).
[16]V. Edelstein, Sol. Stat. Commun. **73**, 233 (1990).
[17]H. B. M. Saidaoui and A. Manchon, Phys. Rev. Lett. **117**, 036601 (2016).
[18]C. O. Avci, K. Garello, I. M. Miron, G. Gaudin, S. Auffret, O. Boulle, and P. Gambardella, Appl. Phys. Lett. **100**, 212404 (2012).
[19]L. Liu, O. J. Lee, T. J. Gudmundsen, D. C. Ralph, and R. A. Buhrman, Phys. Rev. Lett. **109**, 096602 (2012).
[20]X. Zhang, C. H. Wan, Z. H. Yuan, Q. T. Zhang, H. Wu, L. Huang, W. J. Kong, C. Fang, U. Khan, and X. F. Han, Phys. Rev. B **94**, 174434 (2016).
[21]A. Ghosh, K. Garello, C. O. Avci, M. Gabureac, and P. Gambardella, Phys. Rev. Appl. **7**, 014004 (2017).
[22]T. Koyama, Y. Guan, and D. Chiba, Sci. Rep. **7**, 790 (2017).
[23]X. Qiu, W. Legrand, P. He, Y. Wu, J. Yu, R. Ramaswamy, A. Manchon, and H. Yang, Phys. Rev. Lett. **117**, 217206 (2016).
[24]K. Garello, I. M. Miron, C. O. Avci, F. Freimuth, Y. Mokrousov, S. Blugel, S. Auffret, O. Boulle, G. Gaudin, and P. Gambardella, Nat. Nano **8**, 587 (2013).
[25]X. Qiu, P. Deorani, K. Narayanapillai, K.-S. Lee, K.-J. Lee, H.-W. Lee, and H. Yang, Sci. Rep. **4**, 4491 (2014).
[26]M. Yang, K. Cai, H. Ju, K. W. Edmonds, G. Yang, S. Liu, B. Li, B. Zhang, Y. Sheng, S. Wang, Y. Ji, and K. Wang, Sci. Rep. **6**, 20778 (2016).
[27]W. Zhang, V. Vlaminck, J. E. Pearson, R. Divan, S. D. Bader, and A. Hoffmann, Appl. Phys. Lett. **103**, 242414 (2013).
[28]R. M. Rowan-Robinson, A. A. Stashkevich, Y. Roussign, M. Belmeguenai, S.-M. Chrif, A. Thiaville, T. P. A. Hase, A. T. Hindmarch, and D. Atkinson, Sci. Rep. **7**, 16835 (2017).
[29]K.-f. Huang, D.-s. Wang, H.-h. Lin, and C.-h. Lai, Appl. Phys. Lett. **107**, 232407 (2015).
[30]G. Yu, P. Upadhyaya, Y. Fan, J. G. Alzate, W. Jiang, K. L. Wong, S. Takei, S. A. Bender, L.-T. Chang, Y. Jiang, M. Lang, J. Tang, Y. Wang, Y. Tserkovnyak, P. K. Amiri, and K. L. Wang, Nat. Nano **9**, 548 (2014).
[31]K.-S. Lee, S.-W. Lee, B.-C. Min, and K.-J. Lee, Appl. Phys. Lett. **102**, 112410 (2013).
[32]J. Park, G. E. Rowlands, O. J. Lee, D. C. Ralph, and R. A. Buhrman, Appl. Phys. Lett. **105**, 102404 (2014).
[33]S. Azzawi, A. Ganguly, M. Tokaç, R. M. Rowan-Robinson, J. Sinha, A. T. Hindmarch, A. Barman, and D. Atkinson, Phys. Rev. B **93**, 054402 (2016).

[34]M. Tokaç, S. A. Bunyaev, G. N. Kakazei, D. S. Schmool, D. Atkinson, and A. T. Hindmarch, Phys. Rev. Lett. **115**, 056601 (2015).
[35]S. Mizukami, E. P. Sajitha, D. Watanabe, F. Wu, T. Miyazaki, H. Naganuma, M. Oogane, and Y. Ando, Appl. Phys. Lett. **96**, 152502 (2010).
[36]P. F. Carcia, J. Appl. Phys. **63**, 5066 (1988).
[37]S. Mangin, D. Ravelosona, J. A. Katine, M. J. Carey, B. D. Terris, and E. E. Fullerton, Nat. Mater. **5**, 210 (2006).
[38]J. Slonczewski, J. Magn. Magn. Mater. **159**, L1 (1996).
[39]A. Ganguly, R. M. Rowan-Robinson, A. Haldar, S. Jaiswal, J. Sinha, A. T. Hindmarch, D. A. Atkinson, and A. Barman, Appl. Phys. Lett. **105**, 112409 (2014).
[40]J.-C. Rojas-Sánchez, N. Reyren, P. Laczkowski, W. Savero, J.-P. Attané, C. Deranlot, M. Jamet, J.-M. George, L. Vila, and H. Jaffrès, Phys. Rev. Lett. **112**, 106602 (2014).
[41]W. Zhang, W. Han, X. Jiang, S.-H. Yang, and S. S. P. Parkin, Nat. Phys. **11**, 496 (2015).